Magnetodielectric effect in Bi_2NiMnO_6–La_2NiMnO_6 superlattices

2009 J. Phys.: Condens. Matter 21 306004

(http://iopscience.iop.org/0953-8984/21/30/306004)

J. Phys.: Condens. Matter **21** (2009) 306004 (7pp) doi:10.1088/0953-8984/21/30/306004

Magnetodielectric effect in Bi_2NiMnO_6–La_2NiMnO_6 superlattices

P Padhan[1], P LeClair[1,2], A Gupta[1,3], M A Subramanian[4] and G Srinivasan[5]

[1] Materials for Information Technology Center, University of Alabama, Tuscaloosa, Al 35487, USA
[2] Department of Physics and Astronomy, University of Alabama, Tuscaloosa, Al 35487, USA
[3] Department of Chemistry and Department of Chemical and Biological Engineering, University of Alabama, Tuscaloosa, Al 35487, USA
[4] Department of Chemistry and OSUMI, Oregon State University, Corvallis, OR 9733, USA
[5] Physics Department, Oakland University, Rochester, MI 48309, USA

E-mail: agupta@mint.ua.edu

Received 27 May 2009
Published 6 July 2009
Online at stacks.iop.org/JPhysCM/21/306004

Abstract

Multilayer superlattices consisting of multiferroic Bi_2NiMnO_6 (BNMO) and La_2NiMnO_6 (LNMO) have been grown heteroepitaxially on pure and Nb-doped $SrTiO_3$ substrates using the pulsed laser deposition technique. In a series of superlattice structures grown with a fixed BNMO layer thickness of ten unit cells, we find that the *c*-axis lattice parameter, Curie temperature and magnetocapacitance are strongly dependent upon the number of stacked LNMO unit cells in the repeating units. The thickness-dependent magnetodielectric effect is attributed to the fluctuations in electric and magnetic dipole ordering due to the substrate and interface induced stress in the superlattice structures. An enhanced magnetodielectric effect in multilayers with LNMO thicknesses larger than six unit cells is explained based on possible canting of spin at the interfaces of LNMO and BNMO.

(Some figures in this article are in colour only in the electronic version)

1. Introduction

Multilayers that combine ferroelectric and non-ferroelectric materials are very interesting both fundamentally and in terms of their application potential, in particular due to the observation of a strong enhancement of spontaneous polarization, remnant polarization and dielectric constant [1, 2]. Generally, the properties of ferroelectric/non-ferroelectric multilayers appear to be sensitively dependent on various macroscopic geometrical parameters such as layer thicknesses, layering sequence and the ratio of individual layer thicknesses [3, 4]. Multilayers combining ferroelectric and ferromagnetic materials have been investigated only recently [5–7].

Large magnetoelectric effects were observed in multilayers with both ferroelectric and ferromagnetic components [6, 7]. The observed magnetoelectric effects have very specific temperature dependencies, but are rather frequency independent [8]. This can be explained by a spin–lattice coupling, due to an increase of magnetic exchange energy when the magnetic ions shift their positions due to an applied electric field [9]. Various theoretical models have been put forward to explain the role of this intrinsic coupling, the effect of interfacial coupling, and the interfacial strain on ferroelectric superlattices [10, 11].

Multifunctional double perovskite oxides $La_2BB_oO_6$ (B = Ni or Co; B_o = Mn) have recently gained much interest, both because of their rich physics and prospects for technological applications [12]. The compound La_2NiMnO_6 is an ordered double perovskite that is a ferromagnetic semiconductor with a T_{CM} of 280 K. Studies of La_2NiMnO_6 in the bulk have revealed large magnetic field induced changes in the resistivity and dielectric properties at temperatures as high as 280 K [12]. This is a much higher temperature than previously observed for such a coupling between the magnetic, electric, and dielectric properties in a ferromagnetic semiconductor. Substitution at the A site can also lead to multiferroic behaviour in the double perovskites. Azuma *et al* have succeeded in synthesizing the 'designed' compound Bi_2NiMnO_6 in the bulk

under high pressure and established its multiferroic properties, with ferroelectric and ferromagnetic transition temperatures of 485 K and 140 K, respectively [13]. We have synthesized epitaxial thin films of La_2NiMnO_6 [14] and Bi_2NiMnO_6 [15] using the pulsed laser deposition technique, and have reported their magnetodielectric properties [16, 15].

In the present work, we have successfully grown multilayer superlattices of multiferroic La_2NiMnO_6 (LNMO) and Bi_2NiMnO_6 (BNMO), with a view to explore the effects of interfacial coupling and strain within a structurally coherent, fully double perovskite system. In these multilayers, both constituents may exhibit magnetization ordering and polarization ordering, and our previous work has shown magnetodielectric effects in both constituents alone [16, 15]. In a series of LNMO–BNMO superlattices, we have found that *c*-axis lattice parameter, Curie temperature, and magnetocapacitance are strongly dependent upon the relative LNMO layer thickness, and our results suggest that a magnetoelectric effect is intrinsic to LNMO–BNMO multilayers, and may be enhanced by interfacial effects. We also find a correlation between the magnitude of the magnetocapacitance effect and the magnetization of the multilayers.

2. Experimental details

Thin films of Bi_2NiMnO_6 (BNMO), La_2NiMnO_6 (LNMO), and their superlattices were grown on (001)-oriented pure $SrTiO_3$ (STO) and 0.5 wt% Nb-doped $SrTiO_3$ (STNO) substrates using the pulsed laser deposition (PLD) technique. A pulsed KrF excimer laser beam was focused on a $Bi_{2.2}NiMnO_6$ or La_2NiMnO_6 target (nominal composition) to yield energy densities of ∼1.0 and ∼1.5 J cm^{-2}, respectively. The deposition rates per pulse for Bi_2NiMnO_6 and La_2NiMnO_6 (typically ∼0.26 and ∼0.31 Å/pulse, respectively) were calibrated to grow the multilayer heterostructures on STO, placed at a distance of 5 cm from the target, at 730 °C in an ambient oxygen pressure of 800 mTorr. The calibration of the growth rate was established from the superlattice reflections in the θ–2θ x-ray scans of a few test multilayers grown prior to the deposition of the reported multilayer series. After deposition, the samples were cooled to 470 °C in 760 Torr oxygen at 15 °C min^{-1}. The films were subsequently annealed for 1 h at this temperature in the same oxygen pressure, and then cooled to room temperature at 15 °C min^{-1}. The multilayers considered here consisted of ten repetitions of an LNMO/BNMO bilayer, in which the BNMO layer thickness was fixed at 10 unit cells (u.c.), and the LNMO layer thickness t_{LNMO} was varied from 0 to 10 u.c. A final 10 u.c. LNMO capping layer resulted in a series of structures $[(t_{LNMO})LNMO/(10\ u.c.)BNMO]_{10} + 10$ u.c. LNMO.

The epitaxy, superstructure, and crystalline quality of our samples were ascertained using a Philips X'Pert x-ray diffraction (XRD) system. The Bi:La:Ni:Mn ratio in some of the thin film heterostructures was measured using energy dispersive x-ray spectroscopy (EDS), and determined to be close to the desired stoichiometry of 2(Bi + La):1(Ni):1(Mn). Circular 1 mm diameter Au contact pads were sputter deposited on top of the BNMO and STNO to perform two-probe *ac* impedance measurements, with transport along the multilayer growth direction. Impedance (Z) and phase angle (θ) were recorded using a HP4294A impedance analyser as a function of frequency, temperature, and in-plane magnetic field in a Physical Property Measurement System (PPMS, Quantum Design) after cooling the sample down to the desired measurement temperature in the absence of any applied electric or magnetic field.

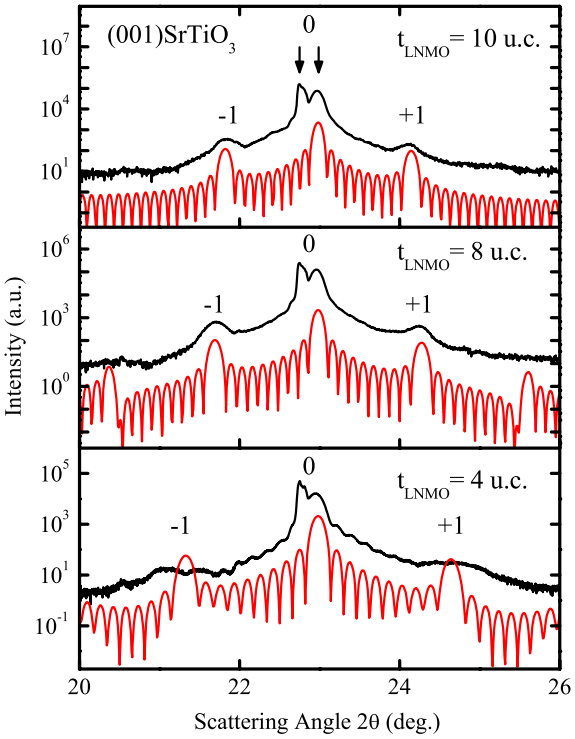

Figure 1. θ–2θ x-ray scan and simulated profile (using the DIFFaX programme) around the (001) reflection of the $[(t_{LNMO})LNMO/(10\ u.c.)BNMO]_{10} + 10$ u.c. LNMO multilayers with $t_{LNMO} = 4$, 8, 10 u.c. grown on (001) oriented $SrTiO_3$ substrates. The lower red curves in each plot are the simulated profiles.

3. Results and discussion

Figure 1 shows the θ–2θ x-ray scans around the (001) diffraction of STO for three multilayer superlattices grown on (001)-oriented STO. The θ–2θ scans clearly show the (001) diffraction peaks of the substrate and the constituents along with the associated superlattice peaks, indicating the growth of an epitaxial pseudo-cubic phase. The multilayer with a 4 u.c. LNMO spacer displays an oscillation of integrated x-ray intensity (i.e. the Pendellösung fringes [17]) in addition to two weak satellite peaks [18] (marked as '+1' and '−1') on either side of its fundamental (001) diffraction peak (marked as '0'). As the LNMO layer thickness increases, the oscillation of integrated intensity is suppressed, but the sharpness of the satellite peaks increases. The presence of satellite peaks clearly demonstrates that a periodically modulated structure has been achieved. The x-ray scans of these multilayers were compared with simulated profiles obtained from the DIFFaX

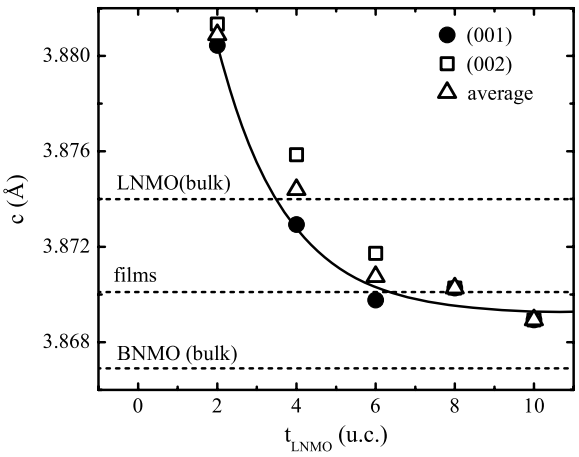

Figure 2. The out-of-plane lattice parameter of multilayers with different LNMO spacer layer thicknesses (t_{LNMO}). The solid line is drawn as a guide to the eye. The dotted lines represent the c axis lattice parameter of bulk LNMO, bulk BNMO, and thin films of either BNMO or LNMO.

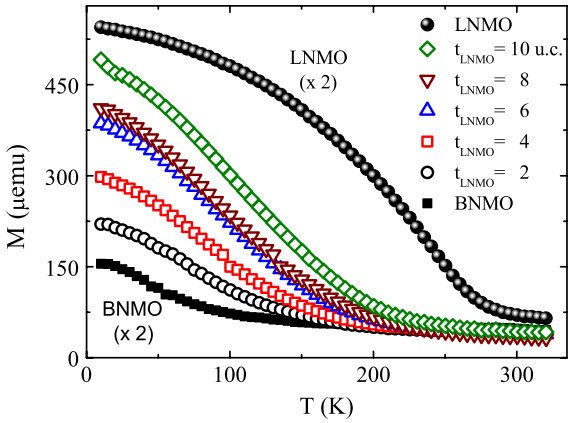

Figure 3. Temperature-dependent cooled magnetization of LNMO, BNMO and the multilayers grown on (001)-oriented STO substrates measured in cooling with an in-plane field of $\mu_0 H_{\mathrm{ext}} = 1.0$ T.

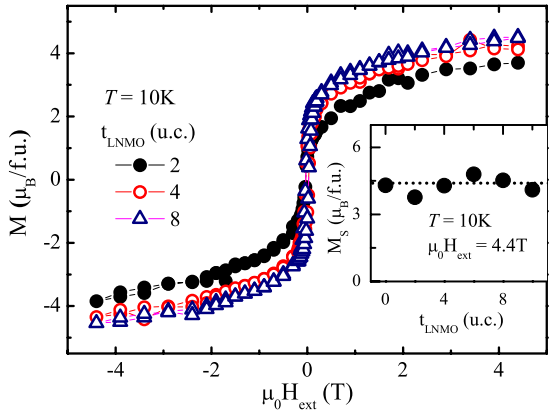

Figure 4. Magnetic hysteresis curves of the multilayers with $t_{\mathrm{LNMO}} = 2$, 4, 8 u.c. at 10 K. The inset shows the magnetization at 4.4 T field versus LNMO thickness t_{LNMO}.

programme [19], also plotted in figure 1. The peak positions and relative intensity ratios of the simulated profile match well with the x-ray scan of the corresponding multilayers.

From the angular position of the fundamental diffraction peak of multilayers, we have calculated their out-of-plane lattice parameters. The change of out-of-plane lattice parameter c of these multilayers with LNMO spacer layer thickness t_{LNMO} is shown in figure 2. The out-of-plane lattice parameter of the multilayer with 2 u.c. thick LNMO spacer layer (3.88 Å) is higher than that of both bulk LNMO (3.874 Å) [12] and BNMO (3.867 Å) [13]. However, as the LNMO spacer layer thickness increases, the out-of-plane lattice parameter of the multilayer decreases, and for 6 u.c. and beyond it is close to that of both bulk BNMO [13] and the value we have found for relatively thick (∼80 u.c.) single LNMO or BNMO films [14, 15]. The pseudo-cubic lattice parameters obtained from the lattice parameter of the bulk monoclinic supercell of LNMO [12] are $a = 3.865$ Å, $b = 3.901$ Å, and $c = 3.874$ Å, while those of the BNMO [13] are $a = 3.821$ Å, $b = 3.936$ Å, and $c = 3.867$ Å. Note that BNMO experiences tensile stress along the 'a' axis and compressive stress along the 'b' axis due to the lattice mismatch with $SrTiO_3$, while LNMO experiences tensile stress along the 'a' axis due to the lattice mismatch with $SrTiO_3$. Thus the strength of the in-plane cumulative stress (i.e. the substrate induced stress and interfacial stress) determine the stress along the c axis. However, the change in the out-of-plane lattice parameter seems to indicate a relaxation of cumulative stress with the increase of LNMO layer thickness.

Figure 3 shows the temperature-dependent field-cooled magnetization $M(T)$ of individual 80 u.c. LNMO and BNMO films and the BNMO–LNMO multilayers. In order to avoid overlapping and to emphasize the transition region of the $M(T)$ curve of the thin films of LNMO and BNMO respectively, we have scaled the observed magnetization for bare LNMO and BNMO films by a factor of two. As the thin film of BNMO was cooled below room temperature in the presence of an in-plane magnetic field of $\mu_0 H_{\mathrm{ext}} = 1.0$ T, its magnetization changes negligibly down to $T = 140$ K. On further cooling, the magnetization increases rapidly down to $T = 50$ K and then remains constant down to the lowest temperature. Similar behaviour of the temperature-dependent magnetization, though with a higher ferromagnetic-to-paramagnetic transition temperature (T_{C}), is observed in the LNMO–BNMO multilayers. Though the T_{C} of the multilayers increases with increasing LNMO thickness, it is significantly smaller than that of a single 80 u.c. LNMO film, presumably due to finite size effects and interfacial coupling with the BNMO.

The zero-field-cooled magnetic hysteresis loops $M(H)$ of three multilayers measured at $T = 10$ K are shown in figure 4 for in-plane applied fields. The shapes of the magnetic hysteresis loops for all multilayers are qualitatively similar, with no significant variation of saturation magnetization, remnant magnetization or coercivity with LNMO layer thickness. As an example, we have shown the magnetization at $\mu_0 H_{\mathrm{ext}} = 4.4$ T for different multilayers in the inset of figure 4. The shapes of the zero-field-cooled hysteresis loops are also reproducible when they are measured after initially cooling the sample in a magnetic field. This reproducibility indicates the absence of any antiferromagnetic coupling [20],

or the formation of antiferromagnetically ordered regions [21] at the interfaces of LNMO and BNMO. From figures 3 and 4 it appears that the alternate stacking of LNMO and BNMO does not significantly influence the temperature- and field-dependent magnetization of the constituents, as is the case for other FM–FM multilayers [22]. Note that in the present multilayer series both FM components are insulating. It is thus expected that the magnetic properties are the result of 180° superexchange interactions between transition metal cations (Goodenough–Kanamori rules) [23], rather than through the double exchange interaction [24] present, for example, in the all-metallic $La_{0.7}Sr_{0.3}MnO_3$–$SrRuO_3$ multilayer system [22].

In order to model the dielectric responses of these multilayers, we first considered the *entire* multilayer as a parallel network of a resistor (R) and a 'leaky' capacitor (C) with a complex dielectric function, $\epsilon(\omega) = \epsilon_1(\omega) + i\epsilon_2(\omega)$, as explained in our previous reports on LNMO [16] and BNMO [15] thin films. In this way, from measurements of impedance and phase angle we can determine the effective capacitance $C_{\rm eff}$ and dissipation factor ($\tan\delta \equiv \epsilon_2/\epsilon_1$) of the multilayer as a whole. In figure 5 we show the temperature-dependent effective capacitance and dissipation factor of several multilayers measured with a 100 mV RMS *ac* voltage at a frequency of $f = 100$ kHz in zero applied magnetic field. Both $C_{\rm eff}$ and $\tan\delta$ show a rapid variation with temperature. In all cases, the dissipation factor of the multilayers increases below room temperature, reaching a maximum at $T \approx 148$ K, and subsequently decreases to a negligible value for lower temperatures down to $T = 4$ K. The effective capacitance decreases monotonically with decreasing temperature from room temperature to $T \sim 100$ K, with a rapid transition at $T \sim 150$ K, below which it remains constant down to $T = 4$ K. We note that the peak in $\tan\delta$ and the rapid decrease of $C_{\rm eff}$ near $T \sim 150$ K shift to slightly higher temperatures as the measurement frequency is increased from 10 to 100 kHz, similar to our earlier observations on single LNMO films [16]. Most notably, for all multilayer samples there is a large variation in capacitance with temperature in a range well below, but in the vicinity of, the onset of magnetic ordering (see figure 3) [15].

Although there is a slight shift of dissipation peak and a corresponding variation in $C_{\rm eff}$ for the multilayers $t_{\rm LNMO} = 2$ u.c., the effective capacitance and dissipation factor show no significant variation in either magnitude or temperature dependence for larger thicknesses. Excepting the multilayers with $t_{\rm LNMO} = 2$ u.c., where slight thickness variations of the extremely thin LNMO spacer may play a more significant role, the lack of a significant thickness dependence argues for a dominant interfacial contribution to the effective capacitance. Since the conductivity of the LNMO–BNMO multilayers decreases rapidly for $T \lesssim 120$ K, as indicated by the temperature dependence of $\tan\delta$, for sufficiently low temperatures the influence of carrier effects on the dielectric properties is expected to be negligible. At higher frequencies, the low-temperature capacitance should therefore provide a measure of the intrinsic permittivities of the constituent layers [25]. If for the moment we assume no interfacial effects, the effective capacitance in that limit would

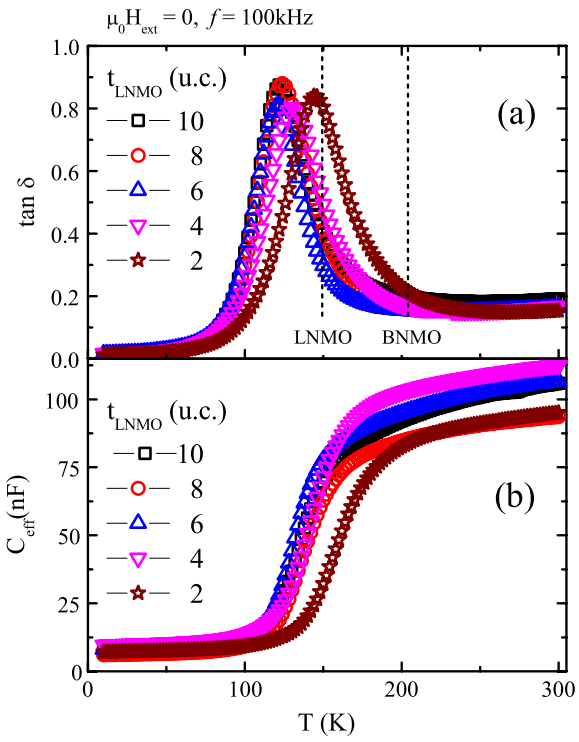

Figure 5. Temperature-dependent (a) dissipation factor $\tan\delta$ and (b) effective capacitance $C_{\rm eff}$ of the multilayers with $t_{\rm LNMO} = 2, 4, 6, 8, 10$ u.c. grown on a (100)-oriented 0.5 wt% Nb-doped STO substrate measured at $f = 100$ kHz. The vertical dashed lines indicate the peak in loss tangent measured for individual BNMO and LNMO films.

simply be a series combination of capacitors representing the individual LNMO and BNMO layers: $C_{\rm eff}^{-1} = n_{\rm BNMO}C_{\rm BNMO}^{-1} + n_{\rm LNMO}C_{\rm LNMO}^{-1}$, where $n_{\rm BNMO} = 10$ and $n_{\rm LMNO} = 11$ are the numbers of BNMO and LNMO layers, respectively. If we further assume that the capacitance of each individual layer scales inversely with its thickness, then the dependence of $C_{\rm eff}^{-1}$ on the LNMO layer thickness $t_{\rm LNMO}$ should show a linear relationship, whose slope and interface give the capacitances for individual LNMO and BNMO layers, respectively. We observe no significant dependence of $C_{\rm eff}$ on $t_{\rm LNMO}$, which suggests that either the interface capacitance or that of the BNMO layers dominates the overall effective capacitance. Based on the effective capacitance measured for relatively thick (~80 u.c.) individual LNMO and BNMO films, we calculate the effective capacitance of a single 10 u.c. BNMO layer as ~40, and ~55 nF for a single 10 u.c. LNMO layer. Using these values, we calculate an effective capacitance for a multilayer with $t_{\rm LNMO} = 10$ u.c. of ~2 nF, roughly two to five times *lower* than the observed value. In the absence of interfacial effects, this alone would suggest an enhancement of the individual LNMO and BNMO dielectric constants by a factor of ~2–5; combined with the lack of a dependence of $C_{\rm eff}$ on $t_{\rm LNMO}$, an interfacial explanation seems in order.

In an attempt to more accurately model the capacitive dielectric response of these multilayers including interfacial effects, we considered each *component* of the multilayer as a parallel combination of a resistor (R) and a 'leaky' capacitor (C) with a complex dielectric function [15, 16]. We further

included a parallel RC contribution for each BNMO–LNMO interface to account for, e.g., interface polarization. Assuming the same value of capacitance for each individual layer and each interface, the effective capacitance of the multilayer can be expressed as $C_{\rm eff}^{-1} = n_{\rm BNMO}C_{\rm BNMO}^{-1} + n_{\rm LNMO}C_{\rm LNMO}^{-1} + n_{\rm int}C_i^{-1}$, where $n_{\rm int} = 20$ is the number of LNMO–BNMO interfaces[6]. Given that the measured effective capacitance is significantly *larger* than expected, however, the series capacitor model only enhances the discrepancy: any interfacial series capacitance will only serve to *lower* the calculated effective capacitance. This suggests either a much larger enhancement of the individual LNMO and BNMO dielectric constants if interfacial effects are to be included in this manner, or an interface polarization opposite to that of the LNMO and BNMO layers—effectively, a negative interface capacitance.

We also note that the $C_{\rm eff}$ determined from our measurements at *room temperature* show a significant discrepancy with the values calculated within a simple RC network model above. In our view, this can attributed to the significant leakage of LNMO and BNMO at higher temperatures. As the temperature is increased from $T = 10$ K, a rapid change of effective capacitance is observed, and the ferroelectric/dielectric behaviour of the multilayer becomes dominated by the strong leakage current. The leaky behaviour is also clearly reflected in a strong reduction of impedance as temperature increases. This is corroborated by an increase in the dissipation factor for higher measurement frequencies. Previously, we observed similar behaviour in individual LNMO films [16].

The *qualitative* behaviour of the temperature-dependent $C_{\rm eff}$ of these multilayers with an applied in-plane magnetic field is similar to the zero field variation shown in figure 5. In the presence of magnetic field, the change in the effective capacitance can be quantified by an effective magnetodielectric constant (MDC), defined by MDC $= [C(\omega, H) - C(\omega, 0)]/C(\omega, 0)$. The MDCs measured at $f = 100$ kHz for various temperatures in an applied in-plane magnetic field of $\mu_0 H_{\rm ext} = 7$ T are shown in figure 6. At $T = 10$ K the MDC of the multilayer with $t_{\rm LNMO} = 2$ u.c. is 0.6%, increasing very slowly with increasing temperature and reaching a maximum at $T \approx 144$ K, thereafter decreasing rapidly to ∼0.1% at $T = 200$ K. Above $T = 200$ K, the variation of the MDC is negligible. Multilayers with larger $t_{\rm LNMO}$ exhibit larger MDC. Again excepting the multilayers with $t_{\rm LNMO} = 2$ u.c. there is no significant change in the peak position with LNMO thickness.

The qualitative behaviour of the $f = 100$ kHz, $\mu_0 H_{\rm ext} = 7$ T MDC of these multilayers is similar to that of its LNMO [16] and BNMO [15] constituents, which has been explained by a coupling between electric and magnetic dipole ordering and fluctuations [16, 15]. The LNMO layer thickness does play a significant role in determining the maximum MDC observed, however. As shown in figure 6(a), with increasing $t_{\rm LNMO}$, the peak in MDC(T) shifts towards lower temperatures,

[6] The LNMO capping layer has a constant thickness of 10 u.c., whereas the other 10 LNMO layers within the repeated LNMO–BNMO bilayer have a variable thickness of $t_{\rm LNMO}$. We have taken this detail into account in the equivalent circuit modelling.

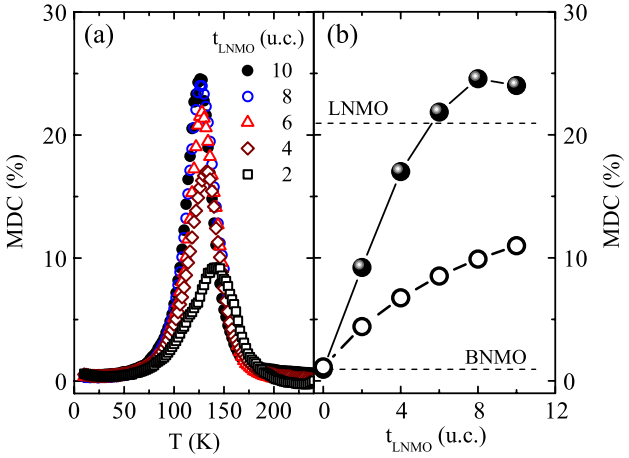

Figure 6. (a) Temperature-dependent magnetodielectric constant MDC of multilayers with $t_{\rm LNMO} = 2, 4, 6, 8, 10$ u.c. grown on a (100)-oriented 0.5 wt% Nb-doped STO substrate measured at $f = 100$ kHz in the presence of 7 T in-plane magnetic field. (b) Maximum MDC of multilayers ● and the expected MDC based on a weighted average of the individual LNMO and BNMO contributions ○ versus LNMO thickness $t_{\rm LNMO}$.

while the maximum MDC itself increases as $t_{\rm LNMO}$ increases from 2 to 6 u.c., approaching saturation for higher thicknesses, as shown in figure 6(b). The dotted lines in figure 6(b) indicate the observed maximum MDC for thin films of BNMO and LNMO alone [16, 15].

The magnitude of the MDC is significantly larger than expected based on the MDC of the individual constituent layers, presuming no interfacial magnetodielectric coupling. The open circles in figure 6(b) are the expected MDC values calculated using a thickness-weighted average of the MDC observed for individual 80 u.c. LNMO and BNMO films [16, 15]. As expected, the measured and calculated MDC increases and shows a tendency toward saturation for larger $t_{\rm LNMO}$, reflecting the relatively larger MDC for individual LNMO layers. The value of the MDC observed for the multilayers, however, is significantly above that expected even for pure LNMO films, again suggesting a significant interfacial magnetodielectric coupling between BNMO and LNMO. Further, the MDC of the multilayers with $t_{\rm LNMO} > 6$ u.c. is essentially independent of the LNMO layer thickness, which also indicates that there is a significant interface magnetoelectric effect independent of the thickness of the LNMO layer. As these multilayers have nominally identical interfaces, the interfacial contribution to the magnetoelectric effect should be same for all multilayers. The thickness variation of MDC below $t_{\rm LNMO} = 6$ u.c. also indicates that the observed magnetoelectric effect is an intrinsic property of this multilayer system. The variation of MDC with LNMO spacer layer thickness is also reminiscent of the thickness dependence of the *stress* along the c axis of the multilayer. The LNMO spacer layer thickness dependent MDC is tentatively attributed to fluctuations in electric dipole ordering and magnetic dipole ordering due to the substrate induced stress and the stress at interfaces. The relatively higher value of MDC of the multilayers with $t_{\rm LNMO} > 6$ u.c. could be a result of the canting

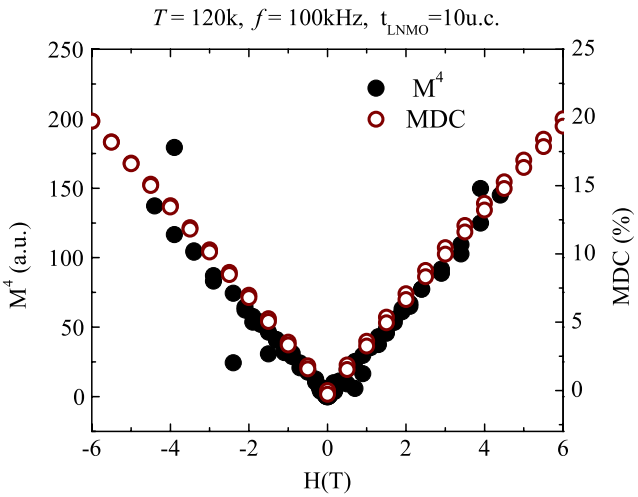

Figure 7. MDC and M^4 versus in-plane magnetic field H for a multilayer with $t_{\mathrm{LNMO}} = 10$ u.c. measured at $T = 120$ K with $f = 100$ kHz.

of spin at the interfaces of LNMO and BNMO [25]. Such non-collinear alignments are very difficult to resolve in magnetic measurements, as despite the number of interfaces the volume fraction is relatively small.

The magnetoelectric effect can be described within the Ginzburg–Landau theory of phase transitions [26, 27, 5], which gives rise to a magnetoelectronic coupling of the form $\gamma P^2 M^2$, where P and M are the polarization and magnetization respectively, and the coupling constant γ is typically a function of temperature [26, 27]. This coupling leads to a deviation of the electric susceptibility, and thus dielectric constant, below the magnetic ordering temperature (T_{C}) as we observe here. If one neglects the temperature dependence of the coupling constant, the resulting variation of the dielectric constant below T_{C} should be proportional to the square of the magnetic order parameter, or in our notation, MDC $\propto M^2$. Indeed, we have previously observed this behaviour for single BNMO layers [15], though it is not obeyed in our single LNMO layers [16]. In the present case, we do not convincingly observe an M^2 dependence, but rather the dielectric constant and MDC appear to follow an M^4 dependence, as shown in figure 7, where both M^4 and MDC are plotted as a function of in-plane magnetic field for a multilayer with $t_{\mathrm{LNMO}} = 10$ u.c., measured at $T = 120$ K with $f = 100$ kHz. Although the possible reasons for this higher-order correlation are unclear, it has been suggested that nonlinear magnetoelectric effects arising from higher-order magnetoelectric coupling terms may be realized in systems with reduced dimensionality [5], in line with our observation of a significant *interface* magnetodielectric effect. Non-collinear spins at BNMO–LNMO interfaces may also play a role in the present case [28].

4. Conclusions

In conclusion we have fabricated multilayers consisting of multiferroic Bi_2NiMnO_6 and ferromagnetic La_2NiMnO_6 double perovskites on pure and Nb-doped $SrTiO_3$ substrates using the pulsed laser deposition technique. The *c*-axis lattice parameter of a series of multilayers with fixed thickness of BNMO strongly depends on the thickness of the LNMO layers. The field-dependent magnetization of these multilayers at $T = 10$ K is independent of LNMO layer thickness, while the Curie temperature increases with increasing LNMO layer thickness. The multilayers grown on conducting Nb-doped $SrTiO_3$ exhibit an enhanced effective capacitance, which is further increased in the presence of magnetic field for a limited temperature range below the magnetic ordering temperature. The maximum magnetocapacitance is strongly dependent upon the LNMO layer thickness, which is attributed to the fluctuations in electric dipole ordering and magnetic dipole ordering due to the substrate induced and interfacial stress. The enhanced magnetodielectric effect of the multilayer with LNMO thicknesses larger than 6 u.c. is potentially explained by the canting of spin at the interfaces of LNMO and BNMO and possibly the effects of reduced dimensionality. Finally, we find that the magnetodielectric effect scales as the fourth power of the magnetization of the multilayers.

Acknowledgments

This work was supported by ONR grant No N000140610226 (C E Wood) and NSF NIRT grant No CMS-0609377. The work performed at Oregon State University is supported by NSF grant (DMR 0804167).

References

[1] Shimuta T, Nakagawara O, Makino T, Arai S, Tabata H and Kawai T 1996 *J. Appl. Phys.* **91** 2290
[2] Erbil A, Kim Y and Gerhardt R 1996 *Phys. Rev. Lett.* **77** 1628
[3] Wang C, Fang Q, Zhu Z, Jiang A, Wang S, Cheng B and Chen Z 2003 *Appl. Phys. Lett.* **82** 2880–2
[4] Harigai T and Tsurumi T 2007 *Ferroelectrics* **346** 56
[5] Eerenstein W, Mathur N D and Scott J F 2006 *Nature* **442** 759–65
[6] Murugavel P, Saurel D, Prellier W, Simon C and Raveau B 2004 *Appl. Phys. Lett.* **85** 4424–6
[7] Kida N, Yamada H, Sato H, Arima T, Kawasaki M, Akoh H and Tokura Y 2007 *Phys. Rev. Lett.* **99** 197404
[8] Scott J 2007 *J. Mater. Res.* **22** 2053
[9] Greenwald S and Smart J 1950 *Nature* **166** 523
[10] Qu D, Zong W and Prince R 1997 *Phys. Rev.* B **55** 11218
[11] Shen J and Ma Y 2000 *Phys. Rev.* B **61** 14279
[12] Rogado N, Li J, Sleight A and Subramanian M A 2005 *Adv. Mater.* **17** 2225
[13] Azuma M, Takata K, Saito T, Ishiwata S, Shimakawa Y and Takano M 2005 *J. Am. Chem. Soc.* **127** 8889
[14] Guo H, Burgess J, Street S, Gupta A, Calvarese T G and Subramanian M A 2006 *Appl. Phys. Lett.* **89** 022509
[15] Padhan P, LeClair P, Gupta A and Srinivasan G 2008 *J. Phys.: Condens. Matter* **20** 355003
[16] Padhan P, Guo H, LeClair P and Gupta A 2008 *Appl. Phys. Lett.* **92** 022909
[17] Padhan P and Prellier W 2007 *Phys. Rev.* B **76** 024427
[18] Padhan P, Prellier W and Mercey B 2004 *Phys. Rev.* B **70** 184419
[19] See http://ccp14.sims.nrc.ca/ccp/ccp14/ftp-mirror/diffax/pub/treacy/DIFFaXIv1807/

[20] Uozu Y, Nakajima T, Nakamura M, Ogimoto Y, Izumi M and Miyano K 2004 *Appl. Phys. Lett.* **85** 2875
[21] Ke X, Rzchowski M, Belenky L and Eom C 2004 *Appl. Phys. Lett.* **84** 5458
[22] Padhan P, Prellier W and Budhani R 2006 *Appl. Phys. Lett.* **88** 192509
[23] Goodenough J 1976 *Magnetism and the Chemical Bond* vol 1 (New York: Interscience) chaper 3
[24] Zener C 1950 *Phys. Rev.* **81** 440
[25] Catalan G, O'Neill D, Bowman R and Gregg J 2000 *Appl. Phys. Lett.* **77** 3078
[26] Kimura T, Kawamoto S, Yamada I, Azuma M, Takano M and Tokura Y 2003 *Phys. Rev.* B **67** 180401
[27] Lawes G, Ramirez A P, Varma C M and Subramanian M A 2003 *Phys. Rev. Lett.* **91** 257208
[28] Scott J F 1977 *Phys. Rev.* B **16** 2329